Prediction of high pressure phases in the systems Li_3N, Na_3N, $(Li,Na)_3N$, Li_2S and Na_2S†

J. Christian Schön, Marcus A. C. Wevers and Martin Jansen

Max-Planck-Institut für Festkörperforschung, Heisenbergstr. 1, D-70569 Stuttgart, Germany. E-mail: schoen@c3serv1.mpi-stuttgart.mpg.de

The prediction of high pressure phases of a chemical system is realized as a two-step process: identification of structure candidates through the global exploration of their energy landscapes over a range of different pressures, followed by a limited local optimization using *ab initio* methods. The application of this recipe is presented for several systems, Li_3N, Na_3N, $Li_xNa_{(6-x)}N_2$ ($x=1,...,5$), Li_2S and Na_2S. We find that at standard pressure, the optimal configurations for the binary end compositions of the alkali nitrides, Li_3N and Na_3N, exhibit the Li_3N and Li_3P structures, respectively. Among the ternary compounds, the compositions with $x=2$ and $x=4$ are preferred, the optimal structures being ternary variations of the Li_3N structure type. At moderately high pressures, phase transitions from Li_3N to Li_3Bi related structures are predicted for all ternary compounds, while Na_3N and Li_3N exhibit transitions from Li_3P to Li_3Bi and Li_3N *via* Li_3P to Li_3Bi, respectively. The analogous study of the landscapes of Li_2S and Na_2S shows that a sequence of phase transitions from the CaF_2 structure *via* the $PbCl_2$ structure to the Ni_2In structure is expected.

1. Introduction

One of the main issues in the field of solid state chemistry is the question: to what extent is it possible to predict which solid compounds are capable of existence in a given chemical system?[1,2] Clearly, one can often provide suggestions based on similar compounds in related systems. With the introduction of high-throughput methods, sometimes collectively called combinatorial chemistry,[3] it has become possible to perform rather systematic explorations of chemical systems. However, this approach is only feasible if the new compounds one aims for are easily accessible *via* a fast massively parallel application of traditional solid state chemistry synthesis techniques.

In most cases, however, synthesizing a new compound is a very challenging task, with even successful syntheses involving many careful experiments. Thus *a priori* information, whether a given chemical system admits the existence of stable or metastable compounds, would be very helpful. An important related issue is the question of whether one should expect phase transitions to occur, *e.g.* due to the application of high pressures or temperatures. Finally, there is the need to determine phase diagrams for ternary or higher compounds. While commonly a few compounds at certain compositions are already known in a given chemical system, there remain large unexplored regions in many phase diagrams.

An obvious alternative to the experimental exploration of a chemical system is the use of theoretical methods, in particular since high-speed computers and more or less robust programs[4–6] for *ab initio* quantum mechanical calculations have become available. Thus, over the past two decades, there have been a number of examples[7,8] where a hypothetical compound has been studied by first choosing a few possible structures by analogy to related systems, then calculating their energies using *ab initio* programs, and finally comparing the results. Depending on the amount of computer time available, the *ab initio*

calculations have also involved some adjustments of the cell constants, yielding an equilibrium volume in the process.

While being very attractive at first sight, this approach still possesses several drawbacks. Most importantly, when guessing the possible structures, one must rely either on one's imagination or on the expectation that nature will repeat itself. Furthermore, these *ab initio* calculations are usually only feasible in the static limit, *i.e.* at $T=0$ K excluding the zero point vibrations; using *ab initio* molecular dynamics at non-zero temperatures is very expensive computationally. Even a local optimization (in the static limit) of both the cell constants and the atomic coordinates is often quite difficult. Thus, in most instances, already estimates of the stability of the hypothetical compounds for non-zero temperatures are not possible, and high-temperature modifications that are not even metastable at low temperatures (*i.e.* that are not associated with a local minimum of the potential energy) are essentially inaccessible.

In order to address these problems, at least to a certain extent, we have developed a multi-stage approach to the prediction of structures of hypothetical compounds.[1] In a first step, a simple empirical potential is employed to approximately model the energy landscape of the chemical system of interest. Next, this energy landscape is explored for a fixed chemical composition using global optimization techniques and related search algorithms. This yields a large set of local minima of the system, each corresponding to a different structure candidate, together with estimates of the energetic and entropic barriers stabilizing these structures. In a further step, these minima serve as input to *ab initio* calculations, where a numerical local optimization of the cell is performed, as far as feasible. Finally, the whole procedure is repeated for many different compositions of the chemical system.

In this paper, we concentrate on the changes of the energy landscape as a function of pressure using lithium nitride as the main example. The results are combined with earlier studies[9,10] of the energy landscapes of alkali metal nitrides in the Li/Na/N system at zero pressure to yield an overview of their stable and metastable compounds as a function of pressure. Finally, results of an analogous study of the landscapes of Li_2S and Na_2S are presented.

---

2. Methods

2.1. Modeling the landscape

In general, many hundreds of global optimization runs have to be performed, in order to find the most important local minima of the energy landscapes of the systems under investigation. Since each run requires several hundred thousand or millions of energy evaluations, it is not possible to employ *ab initio* methods or elaborate computationally intensive potentials at this stage of the procedure. Thus, we model the systems as spherical ions that interact *via* empirical two-body potentials $V_{ij}(r_{ij})$, which only depend on the distances between the ions, r_{ij}. The expression for the enthalpy is

$$H/N = E_{\text{pot}}/N + pV/N = \Sigma_{i<j} V_{ij}(r_{ij}) + pV/N \qquad (1)$$

The potential $V_{ij}(r_{ij})$ consist of three terms: a (screened) Coulomb term for the electrostatic interactions among the ions, a repulsive r^{-12} term, preventing the overlap of the ions, and an attractive r^{-6} term that represents the dispersive interactions:

$$V_{ij}(r_{ij}) = \frac{q_i q_j}{r_{ij}} \exp(-\mu r_{ij}) + \varepsilon_{ij} \left[\left(\frac{\sigma_{ij}}{r_{ij}} \right)^{12} - \left(\frac{\sigma_{ij}}{r_{ij}} \right)^6 \right] \qquad (2)$$

The parameters entering the empirical potential are the sum of the ionic radii multiplied by a scaling factor r_s, $\sigma_{ij} = r_s(r_{\text{ion}}(i) + r_{\text{ion}}(j))$, the parameters ε_{ij}, and the convergence parameter μ. Note that instead of a convergence factor one often employs an Ewald summation in order to compute the electrostatic energy[1,11,12] during the global optimization stage. However, we are predominantly interested in the possible structures and not so much in their actual energies, the latter being computed with *ab initio* methods in a second step. Since our experience shows that using a convergence parameter does not result in different major structure candidates, we have chosen this approach for the purpose of these calculations. Since the effective radius and the strength of the repulsive interaction can vary with pressure or local environment of the ions, it has turned out to be useful[10,12,13] to check the robustness of the local minima found by repeating the global optimizations for slightly different values of ε_{ij}, r_s and μ. In order to achieve a consistent picture in the study presented here, the variation of the landscapes as a function of pressure was performed for fixed parameter values, $\varepsilon_{ij} = \varepsilon = 0.3$, $r_s = 1.1$, and $\mu = 0.15$, which had proven to be suitable in earlier studies‡ at zero pressure.[10] The ionic radii employed during the optimization were r_{ion} (Li$^+$) $= 0.78$ Å, $r_{\text{ion}}(\text{N}^{3-}) = 1.4$ Å, $r_{\text{ion}}(\text{Na}^+) = 0.98$ Å, and $r_{\text{ion}}(\text{S}^{2-}) = 1.94$ Å. For the charges q of the ions, the formal charges were used, $q(\text{Li}^+) = +1$, $q(\text{Na}^+) = +1$, $q(\text{S}^{2-}) = -2$ and $q(\text{N}^{3-}) = -3$.

Since we are interested in crystalline compounds, we have applied periodic boundary conditions. Furthermore, the optimizations were performed for simulation cells that contain either two or four formula units of the respective compounds.

The calculations were repeated for a number of pressures, whose contribution to the enthalpy at $T = 0$ K is given in eqn. (1). Since only a limited number of global optimizations was feasible, we decided to start with a pressure of about one atmosphere, and increase the pressure subsequently by a factor of 10 each time. The reason for this choice of sample pressure was the expectation that at high pressures packing effects would dominate the possible structures, which are controlled by the repulsive terms in the interaction potential (*cf.* eqn. (2)). Thus changes in the landscape between subsequent "high" values of pressure should occur at considerably larger absolute pressure differences than those at "low" pressure values. Of course, in this way one will not be able to calculate *e.g.* a

transition pressure. But at this stage, the goal is only to find structure candidates. No quantitative predictions of phase transitions or ground state energies *etc.* are attempted—the potentials used during the global optimization stage clearly lack the necessary accuracy. Instead, such predictions are based on the subsequent *ab initio* calculations.

2.2. Optimization procedure

The global optimizations were performed using the so-called simulated annealing algorithm,[14,15] which is based on random walks on the energy landscapes. Each step from configuration x_i to a neighbor x_{i+1} is accepted according to the Metropolis criterion, *i.e.* with probability $\min(1, \exp(-(E_{i+1} - E_i)/C))$. Here C is a control parameter, which is reduced to zero, according to a so-called annealing schedule. For a schedule we used $C(n) = C_0 f^n$, $n = 0, ..., n_{\text{max}}$. Typical values were $C_0 = 1.3$ eV atom^{-1}, $f = 0.99$, and $n_{\text{max}} = 1000$, with 300–1000 (depending on the system size) attempted random walk steps between adjustments of C. Typically, the move class (= rule according to which neighboring configurations are chosen at random) was: 80% movements of individual ions, 5% exchanges of ions, and 15% variations of the simulation cell.

One should note that the structure candidates obtained in this way are always slightly distorted from the true structure that usually exhibits at least some symmetry, *i.e.* they are given in the space group $P1$. We have determined the higher symmetry of the true structure using the symmetry finding and space group detecting programs SFND[16] and RGS,[17] respectively.§ The procedure yields idealized structures, which can then be used as input for the cell optimization when performing *ab initio* calculations. Of course, one would prefer to skip this idealization step by performing a full local optimization on an *ab initio* level, including the positions of the individual atoms in addition to the cell parameters. However, even now, such a full optimization is still a very difficult and time-consuming task. Thus, we have optimized only some of the cell parameters of the structure candidates, while keeping the symmetry of the structure and the relative atomic positions fixed.

Of course, even for the same structure, the cell constants and the exact locations of the atoms within the cell vary slightly from run to run, and both depend on pressure. Such variations have commonly been observed during all previous investigations of crystalline systems.[10,12,13] In order to deal with this aspect of global optimization on energy landscapes, we have introduced the concept of a "minimum basin".[18] Such a basin contains all nearly identical local minima that are associated with minute variations of a given structure candidate. These side minima possess tiny energetic barriers and are stabilized by boundary effects due to the long range Coulomb interactions.¶

Furthermore, it is commonly found that several of the structures belonging to distinct minimum basins are nevertheless very closely related in a topological sense.[10,12,13] Their coordination polyhedra and bonding topology are identical, and the configurations can be transformed into each other by very minor changes of the cell parameters together with slight displacements of the atoms. Thus, the structure candidates can be classified according to their topologically different structure types. In most but not all instances, it is obvious which of the several structures associated with the same structure type

---

‡In these studies, ε was varied between 0.1 and 0.5, r_s between 1.0 and 1.2, and μ between 0.05 and 0.15.

§The structure candidates cluster around the high symmetry structure, with deviations $\Delta\phi/\phi$ in angles and $\Delta L/L$ in cell lengths ranging from typically less than 1% up to 5% for strongly distorted minima. In some cases, a sequence of space groups may be found as a function of the tolerances employed in SFND and RGS.

¶These boundary effects are analogous to the surface effects encountered when performing cluster calculations. However, in clusters, these effects can have a physical meaning, while in infinite crystals only an overall dipole moment should survive.[18]

constitute the best minimum and should be chosen as the representative for the *ab initio* calculations.

2.3. *Ab initio* calculations

After performing some preliminary calculations using several *ab initio* methods, the Hartree–Fock method as implemented in the program CRYSTAL95[4] was chosen for the calculation of the alkali nitrides. The test calculations showed[9] both relatively fast convergence and good agreement with experimental values for the cell constants of Li_3N—the only system known in the alkali metal nitrides so far.[19–21] Basis sets were taken from the literature.[22,23] Similarly, for Li_2S and Na_2S, we again used CRYSTAL95, employing basis sets given in the literature,[24,25] where polarization d functions were included for Na and S.

In each system, we calculated the energy as a function of volume for a selected group of structure candidates, varying the volume by *ca.* 1% at each step. During the limited numerical local optimizations involved, the relative positions of the atoms and the symmetry of the structures were kept fixed. Furthermore, for orthorhombic or monoclinic structures, the ratios of the side lengths of the cells were usually not varied, *i.e.* only the total volume was changed during the optimization. The curve $E(V)$ was then found by interpolation, where we have used the standard Murnaghan formula[26]

$$E(V) = \frac{VB_0}{B'_0} \left[\frac{(V_0/V)^{B'_0}}{B'_0 - 1} + 1 \right] - C \qquad (3)$$

Here, the four fit parameters B_0, B'_0, V_0 and C are the bulk modulus and its derivative, the equilibrium volume, and the zero of the energy scale, respectively.

We note that the slope of the $E(V)$ curve for a given structure at some specified volume V' equals the negative value of precisely that pressure $p' = -\partial E/\partial V$, at which V' corresponds to the equilibrium volume of the structure at the pressure p'. As a consequence, the enthalpy $H(p) = E(V(p)) + pV(p)$ is given by the intercept of this tangent with the *y*-axis. Since a pressure-induced phase transition between two structures 1 and 2 implies that both the enthalpies and the pressures are equal in the two phases, $H_1 = H_2$ and $p_1 = p_2 = p_c$, the transition pressure is given by the negative slope of the common tangent of the $E(V)$ curves, $E_{1,2}(V)$, belonging to the two structures. Typically, the error in the computed value of the transition pressure is estimated to be roughly about 20–25%, where three possible sources of error dominate: limitations of the *ab initio* calculations (neglect of correlation energy, choice of basis sets), use of restricted local optimizations when computing data points, and the dependence of the fit of $E(V)$ on the range and density of these data points. If no common tangent exists, or if the tangent implies negative transition pressures, one of the two structures will be metastable at all pressures. One should note, however, that these calculations only apply to zero temperature. It can very well be that for high temperatures, $T \gg 0$, a plot of the respective free energies $F_{1,2}(T;V) = E_{1,2}(T;V) - TS_{1,2}(T;V)$ instead of $E_{1,2}(T=0;V)$ would show a reverse order of the two structures regarding their thermodynamic stability.

3. Results

3.1. Li_3N

3.1.1. Global optimizations at different pressures. Global optimizations in the Li_3N system were performed for nine different pressures: $p = 0$ Pa, 0.16 MPa 1.6 MPa, 16 MPa, 160 MPa, 1.6 GPa, 16 GPa, 160 GPa and 1.6 TPa (0.1 MPa = 1 atm), with 80 simulated annealing runs for each pressure. A certain fraction of the runs did not end up in stable well-defined local minima but ended in amorphous or poorly condensed structures, in particular for "low" pressures,

$p \leqslant 1.6$ GPa. In the subsequent analysis, these runs have been discarded from the statistics. Overall, 42 different structures were found, which could be classified into 23 topologically different structure types.

For each pressure, about the same number of topologically different structure types was found during the global optimizations (7–10). However, for "low" pressures ($p \leqslant 1.6$ GPa), the number of different local minima determined was considerably larger than for "high" pressures ($p \geqslant 16$ GPa): 11–17 *vs.* 7–10, respectively (*cf.* Table 1). Quite generally, $p = 16$ GPa appears to constitute a "watershed" regarding the types of structures observed. With only one exception (I-Na_3N), no structure type was observed both below and above $p = 16$ GPa.

For all pressures, each of the structures exhibited a variation in the enthalpy on the order of 1% from one optimization run to the next. On the other hand, the variability of the unit cell volume for a given structure was much larger at "low" pressures than at "high" pressures (2% *vs.* 0.01%). This difference in variability was also present when an average over all minima observed at a given pressure was performed: both the average volume and the standard deviation decreased with pressure. The reason for the large spread at "low" pressures is connected to a similarly large spread in coordination number of N by Li, of course (*cf.* Table 2). For "low" pressures, the structure candidates exhibited local coordination ranging from $CN = 8$ or 6 to $CN = 14$, with no well-defined structures occurring with $CN = 9$ or 10, however. On the other hand, for "high" pressures the coordination varied much less, $CN = 12$–15. In addition, the fraction of successful optimizations that reached the two most commonly found minimum basins (not always the ones with the lowest energy!) was very high, 65–90%, to be compared with 30–50% at "low" pressures.

An important observation is the fact that for the landscapes at "low" pressure many local minima with rather high energies were found, in agreement with earlier results[10] of global optimizations at $p = 0$ Pa. This suggests that a) the energetic and entropic barriers separating these minima from the rest of the landscape are quite substantial, and b) that the local densities of states in those high lying minimum basins are large enough to compete successfully with the energetically favored low energy minima.** In this context, we note that there exists a large low energy region of the landscape at "low" pressures, where over 80% of all the successful optimization runs ended up. All the structure types belonging to this region can be derived from the Li_3Bi structure type by moderately large rearrangements of the ions, changing the coordination from $8 + 6$ to $11 + 3$, $12 + 2$ or $13 + 1$. Threshold investigations show that these minima are separated by rather small energy barriers that are crossed very quickly, indicating only small entropic contributions to the barriers. Furthermore, their $E(V)$ curves when calculated on an *ab initio* basis are practically identical near the minimum of $E(V)$ (*cf.* Fig. 1). In contrast, all other structure types that occur at "low" pressures appear to be separated by relatively large barriers from the remainder of the landscape. Data for selected structure types are found in the appendix.

3.1.2 *Ab initio* calculations. For the most promising structure types, $E(V)$ curves were computed, and are shown in

---

**Local densities of states $g_i(E)$ refer to the states that belong to the extended region around a minimum i of the energy landscape, which can be determined using *e.g.* the threshold algorithm.[27] These influence the outcome of the global optimization when using *e.g.* simulated annealing starting at high temperatures with a moderately fast schedule. While at $T = 0$ K, the local free energy $F_i = E_i$, where E_i is the potential energy of the local minimum i, for $T > 0$ K, the local entropy $S_i = k_B \ln g_i$ contributes to F_i, $F_i = E_i - TS_i$, and thus minima with large g_i will be sampled frequently during the optimization even for relatively high values of E_i.

Table 1 Number of different structure candidates/structure types that occurred for a given pressure in eV Å^{-3} ($=[16\ \mathrm{GPa}]=[160\ \mathrm{kbar}]$) on the energy landscapes of Li$_3$N, Li$_2$S and Na$_2$S. In parentheses, the percentages of optimization runs that ended in amorphous, very distorted or poorly condensed phases are listed

Pressure	Li$_3$N	Li$_2$S	Na$_2$S
0	15/8 (22%)	4/3 (10%)	5/5 (10%)
0.00001	16/9 (32%)	7/6 (15%)	8/6 (15%)
0.0001	14/7 (26%)	4/3 (20%)	10/7 (15%)
0.001	16/9 (8%)	5/4 (30%)	7/6 (25%)
0.01	17/10 (4%)	6/5 (25%)	9/8 (35%)
0.1	11/8 (6%)	6/4 (50%)	2/2 (5%)
1	10/7 (0%)	3/3 (10%)	2/2 (0%)
10	10/8 (0%)	2/2 (10%)	3/3 (30%)
100	8/7 (0%)	No runs	No runs

Fig. 1. Analyzing these curves, it is found that several phase transitions are feasible for the Li$_3$N system. At $p_c = 0.4 \pm 0.1$ GPa, a transition occurs from the Li$_3$N structure to the Li$_3$P structure, and at $p_c = 27.6 \pm 5.4$ GPa a second transition from the Li$_3$P to the Li$_3$Bi structure. Finally, at extremely high pressures, $p_c = 168 \pm 35$ GPa, a transition to I-Na$_3$N might take place. Furthermore, the ReO$_3$ structure appears to be metastable with a very small transition pressure, $|p_c| < 0.1$ GPa, relative to the Li$_3$N structure. These results confirm and extend earlier investigations,[9] where only three of the structure types (Li$_3$N, Li$_3$P and Li$_3$Bi) found at $p = 0$ Pa had been taken into account.

3.2. Na$_3$N and (Li,Na)$_3$N

In earlier work, the energy landscape of Na$_3$N at zero pressure has been studied in detail.[10] Quite generally, we note that many of the structure types observed for the Li$_3$N system reappeared for the landscape of Na$_3$N. Again many structure candidates related to the Li$_3$Bi structure were found. Using the threshold algorithm,[27] they were shown to be separated by only a small energy barrier (within the empirical potential model, of course). Thus, following the lead of the Li$_3$N system, $E(V)$ curves were calculated only for the Li$_3$N, the Li$_3$P and the Li$_3$Bi structure types[9] (*cf.* Fig. 2). It was found that the structure candidate with the lowest energy at zero pressure is the Li$_3$P structure, closely followed by the Li$_3$N structure. Since the equilibrium volume of the Li$_3$N structure is considerably larger than that of the Li$_3$P structure, it is no surprise that the only pressure induced phase transition found for this system was the one between the Li$_3$P and the Li$_3$Bi structure types at $p_c = 13.8 \pm 3.2$ GPa. The Li$_3$N structure is metastable with a relatively small negative transition pressure, $p_c = -0.3 \pm 0.06$ GPa, relative to the Li$_3$P structure.

Similarly, the energy landscape of the ternary system (Li$_x$Na$_{6-x}$N$_2$) ($x = 1,...,5$) has been studied[9] at zero pressure, and the results can be summarized as follows: At standard pressure, the compositions $x = 2$ and $x = 4$ are preferred, the optimal structures being ternary variations of the Li$_3$N structure type. Here, several of the possible placements of the cations on the Li positions in the Li$_3$N structure are found

to lead to configurations that represent local minima of the energy landscape. In the optimal arrangements, the minority cations are located at the apices of the hexagonal bipyramids around the N ions, connecting the N containing layers. While ternary analogues of the Li$_3$Bi, I-Na$_3$N and Al$_3$Ti structure types are found as additional local minima, no analogues of the Li$_3$P, AuCu$_3$ or Cr$_3$Si structure types have been observed. *Ab initio* calculations show that at moderately high pressures, phase transitions from Li$_3$N to Li$_3$Bi related structures are predicted for all compositions x. However, the transition pressure is much higher ($p_c = 7.8 \pm 1.8$ GPa, $p_c = 7.2 \pm 1.6$ GPa) for the compositions $x = 2$ and 4, respectively, than for the compositions $x = 1,3,5$ ($p_c = 0.3 \pm 0.06$ GPa, $p_c = 2.9 \pm 0.6$ GPa and $p_c = 1.6 \pm 0.35$ GPa, respectively). This serves as an indication that the preference for the compositions $x = 2,4$ should persist towards higher pressures. For comparison, the hypothetical transitions from the Li$_3$N to the Li$_3$Bi structure type for the binary end compositions, the Li$_3$N and the Na$_3$N system, would occur at $p_c = 7.0 \pm 1.5$ GPa and $p_c = 3.0 \pm 0.6$ GPa, respectively.

3.3. Li$_2$S and Na$_2$S

3.3.1. Global optimization runs for Li$_2$S and Na$_2$S at different pressures.
For each of these related energy landscapes, 20 global optimizations were performed for pressures $p = 0$ Pa, 0.16 MPa, 1.6 MPa, 16 MPa, 160 MPa, 1.6 GPa, 16 GPa and 160 GPa each. For half of these runs, two formula units ($Z = 2$) per simulation cell were chosen, and for the other half four formula units ($Z = 4$). A total of 30 different structures were found, which could be classified in 17 structure types. Of these, 11 occurred in the Li$_2$S system (18 different local minima overall), and 16 in the Na$_2$S system (22 different minima overall), with the most important structure candidates present on both landscapes. In general, the same structure candidates were found both for landscapes with $Z = 2$ and for those with $Z = 4$, although a few structures that are based on primitive unit cells containing four formula units were only found in the latter case, of course. The additional freedom in the rearrangements of the atoms in the larger systems was also reflected in slightly smaller ($\Delta V < 1\%$) average volumes and slightly lower average enthalpies of the minimum structures for $Z = 4$ compared with $Z = 2$. Overall, well-defined structures occurred for all coordination numbers between 8 and 12. This differs from the Li$_3$N system, where no well-defined structures with CN = 9, 10 were found. Furthermore, both the spread of coordination numbers (*cf.* Table 2) and the spread in volumes of the structure candidates for a given pressure were considerably smaller than for Li$_3$N. Again, a distinct change in the types of structures that corresponded to local minima of the landscape occurred above a certain pressure, $p = 160$ MPa. Data for selected structure candidates are given in the appendix.

3.3.2 *Ab initio* calculations for Li$_2$S and Na$_2$S.
As for the Li$_3$N system, the most promising structure candidates found

Table 2 Average coordination numbers CN and their spread (in parentheses) for a given pressure in eV Å^{-3} ($=[16\ \mathrm{GPa}]=[160\ \mathrm{kbar}]$) on the energy landscapes of Li$_3$N, Li$_2$S and Na$_2$S

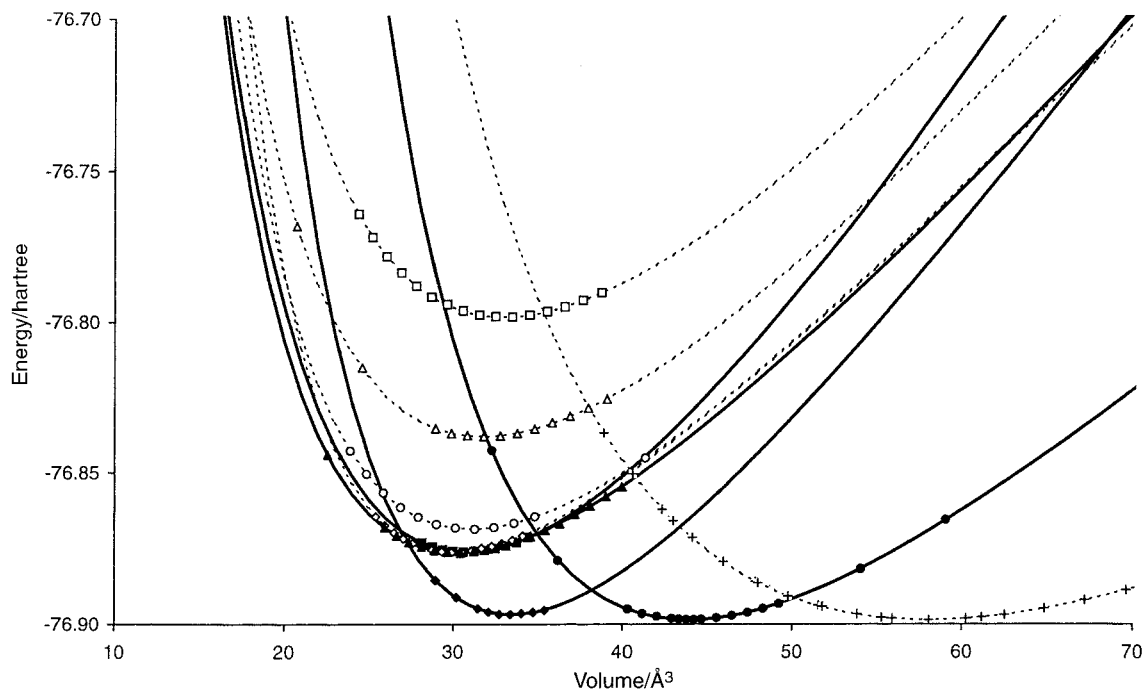| Pressure	Li$_3$N	Li$_2$S	Na$_2$S
0	11.46 (6–14)	8.00 (8–8)	8.33 (8–10)
0.00001	11.40 (6–14)	8.07 (8–9)	8.20 (8–9)
0.0001	11.91 (8–14)	8 (8–8)	8.35 (8–10)
0.001	11.75 (8–14)	8.07 (8–9)	8.40 (8–10)
0.01	11.60 (8–14)	8.07 (8–9)	8.70 (8–11)
0.1	12.16 (11–14)	10.00 (8–11)	11.75 (11–12)
1	12.99 (12–15)	11.70 (10–12)	12.00 (12–12)
10	13.84 (12–15)	12.00 (12–12)	12.00 (12–12)
100	13.65 (12–15)	No runs	No runs

Fig. 1 $E(V)$ curves for promising structure candidates (*cf.* Table A1 in the appendix) in the system Li_3N. Li_3N: filled circles (solid), Li_3P: filled diamonds (solid), ReO_3: crosses (dashed), Li_3Bi: filled triangles (solid), I-Na_3N: filled squares (solid), Al_3Ti: hollow diamonds (dashed), Cr_3Si: hollow circles (dashed), $AuCu_3$: hollow squares (dashed), A1-Li_3N: hollow triangles (dashed). The computed data points used for the Murnaghan fit are shown for each curve. Structures that are found to be stable in some pressure range are shown as solid curves, while the metastable ones are given as dashed lines.

for Li_2S were chosen for refinement optimizations. The corresponding $E(V)$ curves are shown in Fig. 3. We see that for Li_2S a phase transition should occur at a pressure of about $p_c = 24 \pm 6$ GPa from the CaF_2 (CN = 8) to the $PbCl_2$ structure (CN = 9), followed by another from the $PbCl_2$ to the Ni_2In structure (CN = 11) at $p_c = 42 \pm 9$ GPa. Several high pressure structure candidates with even higher coordination numbers like the A1-Li_2S structure (hexagonal $Na_{12}S$ prisms, space group $P6/mmm$) have also been investigated, but so far it appears that no further transition should occur up to 1 TPa.

Similar to the Li_2S system, we have also performed *ab initio* local optimizations for Na_2S. The results available so far indicate that a phase transition should occur between the CaF_2 and the Ni_2In structure, with a possible appearance of the $PbCl_2$ structure over a short intermediate pressure range. This might be followed by a transition to a 12-fold coordinated structure A1-Na_2S (space group $I4_1/amd$) at very high pressures. The transition pressure(s) for the transition(s) up to the Ni_2In structure are expected to lie in a pressure range around $p_c = 11 \pm 2.5$ GPa, while either the A1-Na_2S structure
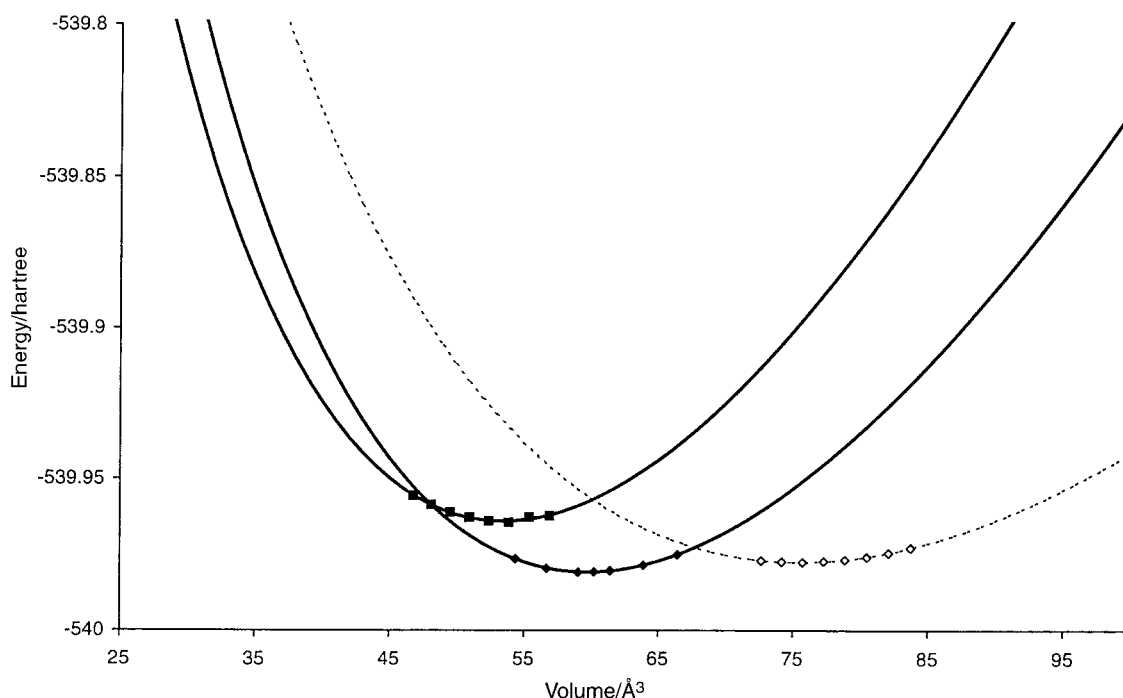

Fig. 2 $E(V)$ curves for promising structure candidates (*cf.* Table A2 in the appendix) in the system Na_3N. Li_3N: hollow diamonds (dashed), Li_3P: filled diamonds (solid), Li_3Bi: filled squares (solid). The computed data points used for the Murnaghan fit are shown for each curve. Structures that are found to be stable in some pressure range are shown as solid curves, while the metastable ones are given as dashed lines.
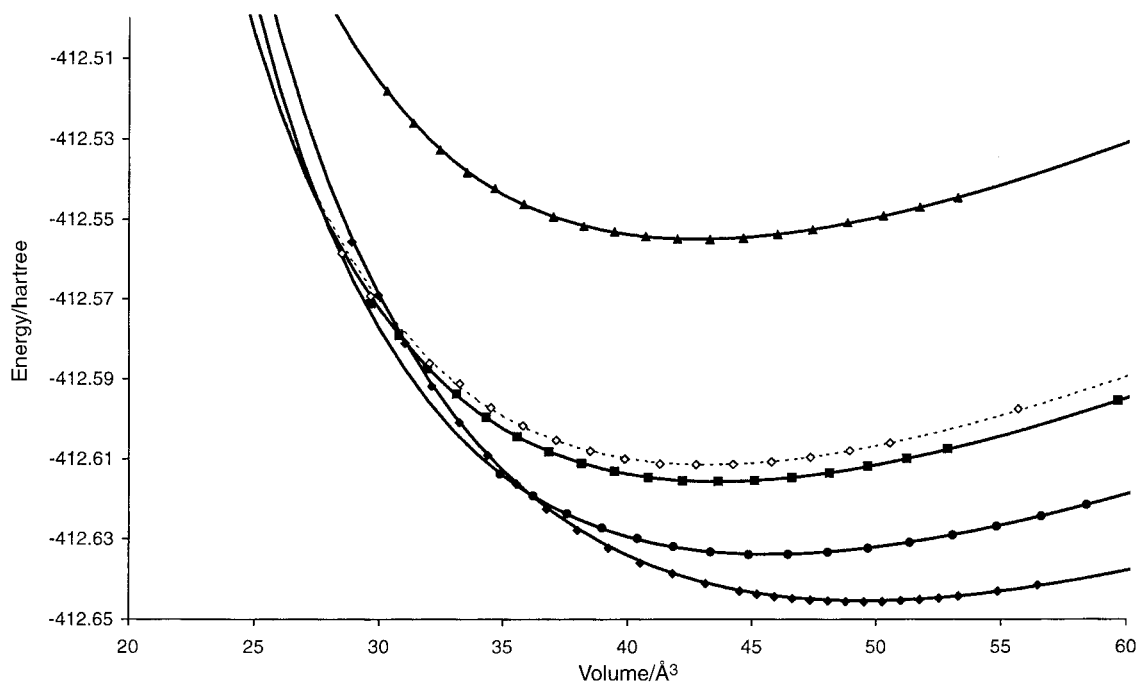
Fig. 3 $E(V)$ curves for promising structure candidates (*cf.* Table A3 in the appendix) in the system Li$_2$S. CaF$_2$: filled diamonds (solid), PbCl$_2$: filled circles (solid), Ni$_2$In: hollow diamonds (dashed), Ni$_2$In-(d) (see Discussion): filled squares (solid), A1-Li$_2$S: filled triangles (solid). The computed data points used for the Murnaghan fit are shown for each curve. Structures that are found to be stable in some pressure range are shown as solid curves, while the metastable ones are given as dashed lines.

or the A2-Na$_2$S structure might be stable above a pressure of $p_c = 120$ GPa.

4. Discussion

Perhaps the most striking result of the landscape investigations is the persistence of major features of the energy landscape when varying the pressure. Many of the important structure types correspond to deep-lying local minima over a wide pressure range, for both alkali metal nitrides and sulfides. The second general observation is the division of the structures into two groups, constituting local minima at either "high" or "low" pressures. This is no great surprise, of course, but it underlines the importance of exploring the energy landscape of a system at many different pressures.

When comparing the landscapes for different systems, it appears somewhat surprising that considerably more structure candidates are found for Li$_3$N than for Li$_2$S and Na$_2$S taken together. However, this might well be caused by the larger sample of optimization runs for the Li$_3$N system. Clearly, further optimizations are needed for the sulfides, which might result in a change in the number of distinct structures observed.

As was mentioned earlier, Li$_3$N is the only binary or ternary alkali metal nitride known so far. Its high pressure behavior has been studied in recent years, and the transition to the Li$_3$P structure we have found has been observed at *ca.* 0.6 GPa[28] by experiment. Taking into account experimental and theoretical uncertainties, this agrees well with the value of 0.4 GPa we have computed. Furthermore, there are hints at a transition to a high-symmetry structure like *e.g.* Li$_3$Bi somewhere in the pressure range from 10 to 35 GPa.[28,29] Again, this agrees well with our prediction of a transition to Li$_3$Bi or a closely related structure at $p_c = 28$ GPa. Clearly, more careful experimental investigations are needed to resolve the discrepancy between the experiments and allow a comparison with our calculations. We also note that our results are of the same order of magnitude as those of a recent LDA-based calculation[29] for Li$_3$N, where a transition pressure of 38 GPa has been suggested between the Li$_3$P structure (which was computed to be the

equilibrium structure at standard pressure, however!) and the Li$_3$Bi structure.

Regarding Na$_3$N and the ternary system (Li,Na)$_3$N, no synthesis has proven to be successful so far, in spite of some claims in the past.[30] Thus we can only judge the results by comparing with the most closely related structures. Here, the fact that the energy landscapes of Li$_3$N and Na$_3$N are very similar lends confidence to the prediction of Na$_3$N existing either in the Li$_3$N or the Li$_3$P structure at standard pressure. For the ternary system, we note that in particular the Li$_3$N related structures with minority cations at the apices of the hexagonal bipyramids lead to very well balanced structures for Li : Na ratios of 1 : 2 ($x = 2$) and 2 : 1 ($x = 4$). As a consequence, we might find phase separation instead of perfect mixing in the (Li,Na)$_3$N system. The preference for the Li$_3$N related modifications at standard pressure agrees well with the existence of ternary systems[31–33] of the composition (Li,M)$_3$N (M = Cu, Ni, Co, Mn, Fe), all exhibiting a Li$_3$N related structure with minority cations between the layers containing N ions.

While this is very encouraging, one needs to recall that in general further phases might be present that do not show the desired composition (Li,Na)$_3$N. In particular, elementary (gaseous) nitrogen and (metallic) sodium together with Li$_3$N might form as an alternative to the desired compounds, *e.g.* Li$_2$NaN or LiNa$_2$N.

Turning to the sulfides, recent experimental work[34] on Li$_2$S has shown that the transition to the PbCl$_2$ structure type does take place at $p_c = 12$ GPa, while the predicted transition to the Ni$_2$In structure at higher pressure has not yet been observed. Regarding experiments on Na$_2$S, transitions from the CaF$_2$ structure *via* the PbCl$_2$ structure to the Ni$_2$In structure have recently been observed[35] at pressures of about 5 GPa, and somewhere between 8 and 20 GPa, respectively, while further transitions at higher pressures have not yet been found.

In this context one needs to address the question of systematic errors in the qualitative and quantitative prediction of transition pressures. Beyond the basic limitations of each *ab initio* method, we face the requirement of having to use the same basis set and/or effective interaction potential for all

volumes, in order to achieve consistency and comparability of the $E(V)$ curves. This can lead to various cut-off problems when computing data points far away from the minimum of the $E(V)$ curve. This is especially critical when starting from structure candidates that were only observed at high pressures, since here the starting point of the local optimization can be far removed from the minimum of the $E(V)$ curve. While this has not been a problem for the sulfides up to now, it has proven to be rather difficult to achieve convergent $E(V)$ calculations for the structure candidates found at very high pressures ($p \geqslant 160$ GPa) in the Li$_3$N system. Thus these data have been excluded from the $E(V)$ diagram in Fig. 1. A further potential source of error is the dependence of the fit on the available computed data points, especially when attempting extrapolations towards low volumes. Tests for *e.g.* the sulfide systems have shown that the curvature of the fitted $E(V)$ curve can exhibit non-negligible changes upon addition of further data points.

A second concern is the restriction of keeping symmetry and atomic positions fixed during the local optimizations with *ab initio* methods. As a consequence, the computations produce at best upper bounds on the true $E(V)$ curves of the compound. This *caveat* applies in particular if the structure under investigation is not highly symmetric or contains many atoms in general positions (x,y,z). Since we are rarely able to optimize all cell parameters and the positions of the atoms at the same time, it is quite likely that in such a case the true $E(V)$ curve will lie somewhat lower than the computed one, resulting *e.g.* in a lower transition pressure. Directly related to this is the fact that a numerical optimization by hand (CRYSTAL95 has no gradient available) will always lack the precision of a gradient based optimization. An instance where a full optimization might be advisable is the PbCl$_2$ related structure found in Li$_2$S and Na$_2$S, which possesses a relatively low symmetry and contains many atoms in general positions, and is similar in energy to the Ni$_2$In structure in Na$_2$S. Thus, the corresponding $E(V)$ curves computed for Li$_2$S (Fig. 3) and Na$_2$S (Fig. 4) should only be considered as a first approximation as far as quantitative conclusions are concerned.
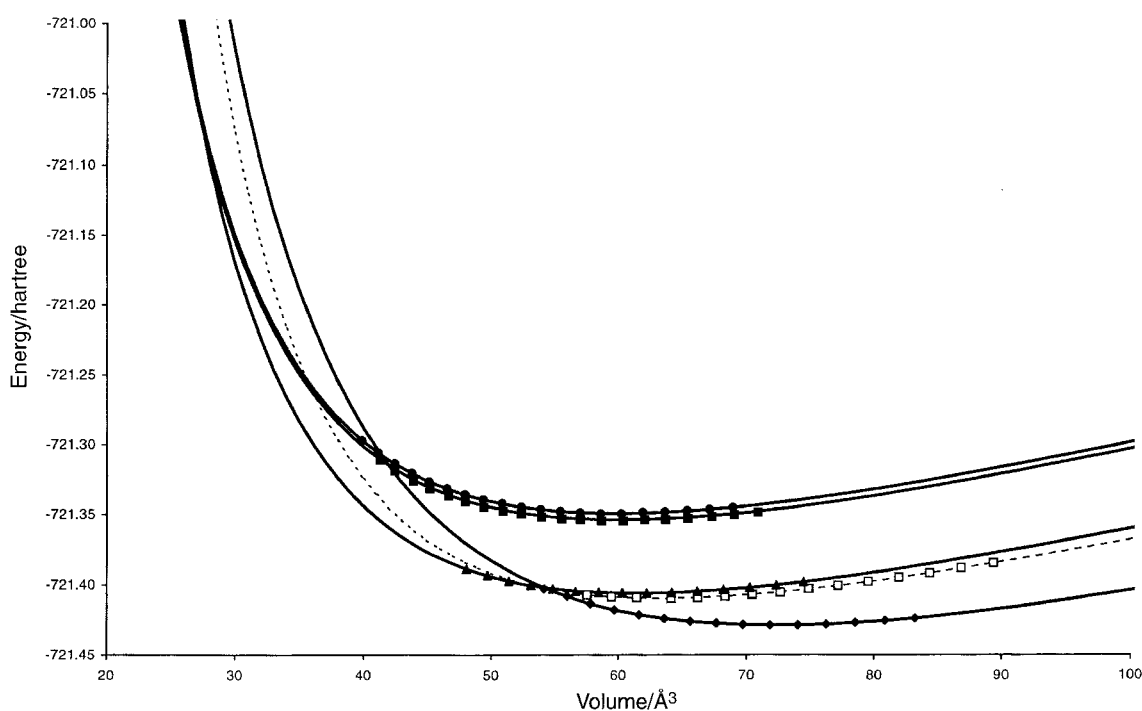
In order to investigate the possible errors due to an incomplete local optimization, we have computed additional $E(V)$ data points, both for Li$_2$S and Na$_2$S in the Ni$_2$In and the PbCl$_2$ modifications each. We find for most modifications, except for the PbCl$_2$ structure in Li$_2$S, that the data points resulting from the less restricted local optimization lie clearly below the curve obtained from the one-parameter optimization. Furthermore, there appears to be a slight shift to somewhat larger equilibrium volumes at zero pressure. In addition, we also studied the effect of including five more data points at low volumes for the fluorite structure of Na$_2$S. We find that the curvature of the $E(V)$ curve changes significantly, leading to a large change of the transition pressure from 16 GPa to about 11 GPa. In general one should note that the effect of the potential errors appears to be very specific for each system and modification. Furthermore, the changes in the $E(V)$ curve have the greatest impact in the range of very small volumes and extremely high pressures ($p > 10$ GPa).

Finally, we note that it is quite possible that a slightly distorted structure candidate with somewhat lower symmetry might be energetically preferable within some pressure range. An example is the Ni$_2$In structure type in Li$_2$S, which occurred as a local minimum both as a fully symmetric and a slightly distorted structure, called Ni$_2$In and Ni$_2$In-(d), respectively. For both, the $E(V)$ curves have been computed and are shown in Fig. 3. We note that in this instance, the distorted version appears slightly more favorable at low pressures, while at high pressures both curves are nearly identical.

5. Summary

We have shown how a two-step procedure consisting of an exploration of the energy landscapes of chemical systems at various pressures using global optimization techniques, followed by a local optimization with *ab initio* methods, leads to successful predictions of pressure induced phase transitions. For those chemical systems where a synthesis has already been successful (Li$_3$N, Li$_2$S, Na$_2$S), the results agree well with experimental observations. But there still remains a

Fig. 4 $E(V)$ curves for promising structure candidates (*cf.* Table A4 in the appendix) in the system Na$_2$S. CaF$_2$: filled diamonds (solid), PbCl$_2$: hollow squares (dashed), Ni$_2$In: filled triangles (solid), A1-Na$_2$S: filled circles (solid), A2-Na$_2$S: filled squares (solid). The computed data points used for the Murnaghan fit are shown for each curve. Structures that are found to be stable in some pressure range are shown as solid curves, while the metastable ones are given as dashed lines.

challenge to the experimentalist, as additional predicted structures in the Li_3N, Na_3N, $(Li,Na)_3N$, Li_2S and Na_2S systems still await their realization.

Appendix

Table A1: Structure candidates for Li_3N that were selected for *ab initio* calculations

Li_3N Minimum	Space group (number), origin choice, crystal system	Lattice constants a, b, c/Å; α, β, γ/°	Atom (multiplicity, Wyckoff symbol), fractional coordinates			
Li_3N	*P6/mmm* (191), hexagonal	$a=3.612$, $c=3.875$ $\alpha=90.00$, $\beta=90.00$, $\gamma=120.00$	Li2 (2c)	1/3	2/3	0
			Li1 (1b)	0	0	1/2
			N (1a)	0	0	0
I-Na_3N	*Pmmn* (59), orthorhombic	$a=3.523$, $b=4.929$, $c=3.523$ $\alpha=90.00$, $\beta=90.00$, $\gamma=90.00$	Li1 (4e)	3/4	0.5	0.72
			Li2 (2b)	3/4	1/4	0.18
			N (2a)	3/4	3/4	0.78
Al_3Ti	*I4/mmm* (139), tetragonal	$a=3.502$, $c=4.877$ $\alpha=90.00$, $\beta=90.00$, $\gamma=90.00$	Li1 (4d)	1/2	0	1/4
			Li2 (2b)	1/2	1/2	0
			N (2a)	0	0	0
Li_3P	*P6₃/mmc* (194), origin choice 2, hexagonal	$a=3.509$, $c=6.262$ $\alpha=90.00$, $\beta=90.00$, $\gamma=120.00$	Li1 (4f)	1/3	2/3	0.58
			N (2c)	1/3	2/3	1/4
			Li2 (2b)	0	0	0
Li_3Bi	*Fm$\bar{3}$m* (225), cubic	$a=4.957$ $\alpha=90.00$, $\beta=90.00$, $\gamma=90.00$	Li (8c)	1/4	1/4	1/4
			N (4b)	1/2	1/2	1/2
			Li (4a)	0	0	0
$AuCu_3$	*Pm$\bar{3}$m* (221), cubic	$a=3.223$ $\alpha=90.00$, $\beta=90.00$, $\gamma=90.00$	Li (3c)	1/2	1/2	0
			N (1a)	0	0	0
Cr_3Si	*Pm$\bar{3}$n* (223), cubic	$a=3.967$ $\alpha=90.00$, $\beta=90.00$, $\gamma=120.00$	Li (6c)	1/4	0	1/2
			N (2a)	0	0	0
ReO_3	*Pm$\bar{3}$m* (221), cubic	$a=4.334$ $\alpha=90.00$, $\beta=90.00$, $\gamma=90.00$	Li (3d)	1/2	0	0
			N (1a)	0	0	0
A1-Li_3N	*Cmma* (67), orthorhombic	$a=3.972$, $b=5.956$, $c=5.372$ $\alpha=90.00$, $\beta=90.00$, $\gamma=90.00$	Li (8m)	0	0.10	0.64
			N (4g)	1/2	1/4	0.74
			Li (4a)	1/4	1/2	0

Table A2: Structure candidates for Na_3N that were selected for *ab initio* calculations

Na_3N Minimum	Space group (number), origin choice, crystal system	Lattice constants a, b, c/Å; α, β, γ/°	Atom (multiplicity, Wyckoff symbol), fractional coordinates			
Li_3P	*P6₃/mmc* (194), origin choice 2, hexagonal	$a=4.257$, $c=7.524$ $\alpha=90.00$, $\beta=90.00$, $\gamma=120.00$	Li1 (4f)	1/3	2/3	0.58
			N (2c)	1/3	2/3	1/4
			Li2 (2b)	0	0	0
Li_3N	*P6/mmm* (191), hexagonal	$a=4.365$, $c=4.590$ $\alpha=90.00$, $\beta=90.00$, $\gamma=120.00$	Li2 (2c)	1/3	2/3	0
			Li1 (1b)	0	0	1/2
			N (1a)	0	0	0
Li_3Bi	*Fm$\bar{3}$m* (225), cubic	$a=5.995$ $\alpha=90.00$, $\beta=90.00$, $\gamma=90.00$	Li (8c)	1/4	1/4	1/4
			N (4b)	1/2	1/2	1/2
			Li (4a)	0	0	0

Table A3: Structure candidates for Li_2S that were selected for *ab initio* calculations

Li_2S Minimum	Space group (number), origin choice, crystal system	Lattice constants a, b, c/Å; α, β, γ/°	Atom (multiplicity, Wyckoff symbol), fractional coordinates			
CaF_2	*Fm$\bar{3}$m* (225), cubic	$a=5.5$ $\alpha=90.00$, $\beta=90.00$, $\gamma=90.00$	Li (8c)	1/4	1/4	1/4
			S (4a)	0	0	0
Ni_2In-(d) distorted, see text	*Cmcm* (63), orthorhombic	$a=4.065$, $b=7.870$, $c=5.458$ $\alpha=90.00$, $\beta=90.00$, $\gamma=120.00$	Na1 (4c)	0	0.67	1/4
			S (4c)	1/2	0.85	1/4
			Na2 (4a)	0	0	1/2
Ni_2In	*P6₃/mmc* (194), hexagonal	$a=4.350$, $c=5.220$ $\alpha=90.00$, $\beta=90.00$, $\gamma=120.00$	S (2d)	1/3	2/3	3/4
			Li1 (2c)	1/3	2/3	1/4
			Li2 (2a)	0	0	0
A1-Li_2S	*P6/mmm* (191), hexagonal	$a=3.824$, $c=3.635$ $\alpha=90.00$, $\beta=90.00$, $\gamma=120.00$	Li (2d)	2/3	1/3	1/2
			S (1a)	0	0	0
$PbCl_2$	*Pnma* (62), orthorhombic	$a=6.278$, $b=3.828$, $c=7.470$ $\alpha=90.00$, $\beta=90.00$, $\gamma=90.00$	Li1 (4c)	0.97	3/4	0.67
			Li2 (4c)	0.64	1/4	0.57
			S (4c)	0.25	1/4	0.61

Table A4: Structure candidates for Na$_2$S that were selected for *ab initio* calculations

Na$_2$S Minimum	Space group (number), origin choice, crystal system	Lattice constants a, b, c/Å; α, β, γ/°	Atom (multiplicity, Wyckoff symbol), fractional coordinates			
CaF$_2$	$Fm\overline{3}m$ (225), cubic	$a = 6.600$	Na (8c)	1/4	1/4	1/4
		$\alpha = 90.00$, $\beta = 90.00$, $\gamma = 90.00$	S (4a)	0	0	0
Ni$_2$In	$P6_3/mmc$ (194), hexagonal	$a = 4.915$, $c = 5.950$	S (2d)	1/3	2/3	3/4
		$\alpha = 90.00$, $\beta = 90.00$, $\gamma = 120.00$	Na1 (2c)	1/3	2/3	1/4
			Na2 (2a)	0	0	0
A1-Na$_2$S	$I4_1/amd$ (141), origin choice 2, tetragonal	$a = 3.755$, $c = 13.202$	Na (8e)	1/2	1/4	0.21
		$\alpha = 90.00$, $\beta = 90.00$, $\gamma = 90.00$	S (4b)	0	1/4	7/8
A2-Na$_2$S	$P6/mmm$ (191), hexagonal	$a = 3.816$, $c = 3.696$	Na (2d)	2/3	1/3	1/2
		$\alpha = 90.00$, $\beta = 90.00$, $\gamma = 120.00$	S (1a)	0	0	0
PbCl$_2$	$Pnma$ (62), orthorhombic	$a = 6.278$, $b = 3.828$, $c = 7.470$	Na1 (4c)	0.71	1/4	0.42
		$\alpha = 90.00$, $\beta = 90.00$, $\gamma = 90.00$	Na2 (4c)	0.95	3/4	0.30
			S (4c)	0.27	3/4	0.89

References

1 J. C. Schön and M. Jansen, *Angew. Chem.*, 1996, **108**, 1358; J. C. Schön and M. Jansen, *Angew. Chem., Int. Ed. Engl.*, 1996, **35**, 4001.
2 M. L. Cohen, *Science*, 1986, **234**, 549.
3 B. Jandeleit, D. J. Schaefer, T. S. Powers, H. W. Turner and W. H. Weinberg, *Angew. Chem.*, 1999, **111**, 1648; B. Jandeleit, D. J. Schaefer, T. S. Powers, H. W. Turner and W. H. Weinberg, *Angew. Chem., Int. Ed.*, 1999, **38**, 2494.
4 R. Dovesi, V. R. Saunders, C. Roetti, M. Causa, N. M. Harrison, R. Orlando and E. Apra, CRYSTAL95, University of Torino, 1996.
5 P. Blaha, K. Schwarz and J. Luitz, WIEN97, Vienna University of Technology, 1997.
6 R. Car and M. Parinello, *Phys. Rev. Lett.*, 1985, **55**, 2471.
7 A. Y. Liu and M. L. Cohen, *Phys. Rev. B*, 1990, **41**, 10727.
8 P. Kroll and R. Hoffmann, *Angew. Chem., Int. Ed.*, 1998, **37**, 2527.
9 J. C. Schön, M. A. C. Wevers and M. Jansen, *Solid State Sci.*, 2000, in press.
10 M. Jansen and J. C. Schön, *Z. Anorg. Allg. Chem.*, 1998, **624**, 533.
11 S. W. DeLeeuw, J. W. Perram and E. R. Smith, *Proc. R. Soc. London A*, 1980, **373**, 27.
12 M. A. C. Wevers, J. C. Schön and M. Jansen, *J. Solid State Chem.*, 1998, **136**, 233.
13 J. C. Schön and M. Jansen, *Comput. Math. Sci.*, 1995, **4**, 43.
14 S. Kirkpatrick, C. D. Gelatt, Jr. and M. P. Vecchi, *Science*, 1983, **220**, 671.
15 V. Czerny, *J. Opt. Theory Appl.*, 1985, **45**, 41.
16 R. Hundt, J. C. Schön, A. Hannemann and M. Jansen, *J. Appl. Crystallogr.*, 1999, **32**, 413.
17 A. Hannemann, R. Hundt, J. C. Schön and M. Jansen, *J. Appl. Crystallogr.*, 1998, **31**, 922.
18 M. A. C. Wevers, J. C. Schön and M. Jansen, *J. Phys. Condens. Matter*, submitted.
19 E. Zintl and G. Brauer, *Z. Electrochem.*, 1935, **41**, 102.
20 A. Rabenau and H. Schulz, *J. Less-Common Met.*, 1976, **50**, 155.
21 N. E. Brese and M. O'Keefe, *Struct. Bonding (Berlin)*, 1992, 307.
22 M. Prencipe, A. Zupan and R. Dovesi, *Phys. Rev. B*, 1995, **51**, 3391.
23 R. Pandey, J. E. Jaffe and N. M. Harrison, *J. Phys. Chem. Solids*, 1994, **55**, 1357.
24 A. Lichanot, E. Apra and R. Dovesi, *Phys. Status Solidi (b)*, 1993, **177**, 157.
25 R. Dovesi, C. Roetti, C. Freyria-Fava, M. Prencipe and V. R. Saunders, *Chem. Phys.*, 1991, **156**, 11.
26 F. D. Murnaghan, *Proc. Natl. Acad. Sci. USA*, 1944, **30**, 244.
27 J. C. Schön, H. Putz and M. Jansen, *J. Phys. Condens. Matter*, 1996, **8**, 143.
28 H. J. Beister, S. Haag, R. Kniep, K. Strößner and K. Syassen, *Angew. Chem.*, 1988, **100**, 1116.
29 A. C. Ho, M. K. Granger and A. L. Ruoff, *Phys. Rev. B*, 1999, **59**, 6083.
30 H. Wattenberg, *Ber. Dtsch. Chem. Ges.*, 1930, **63**, 1667.
31 W. Sachsze and R. Juza, *Z. Anorg. Allg. Chem.*, 1949, **259**, 278.
32 J. Klatyk and R. Kniep, *Z. Kristallogr. NCS*, 1999, **214**, 447.
33 J. Klatyk and R. Kniep, *Z. Kristallogr. NCS*, 1999, **214**, 445.
34 A. Grzechnik, A. Vegas, K. Syassen, I. Loa, M. Hanfland and M. Jansen, *J. Solid State Chem.*, 2000, in press.
35 A. Vegas, A. Grzechnik, K. Syassen, I. Loa, M. Hanfland and M. Jansen, *Acta Crystallogr., Sect. B*, submitted.